Enzyme-Catalyzed Polymerization of 8-Hydroxyquinoline-5-sulfonate by *In Situ* Nuclear Magnetic Resonance Spectroscopy

K. SHRIDHARA ALVA, LYNNE SAMUELSON, JAYANT KUMAR, SUKANT TRIPATHY, ASHOK L. CHOLLI

Departments of Chemistry and Physics, Center for Advanced Materials, University of Massachusetts Lowell, Lowell, Massachusetts 01854

Received 2 September 1997; accepted 27 January 1998

ABSTRACT: In this report, we describe the use of *in situ* NMR spectroscopy to elucidate the mechanism of horseradish peroxidase-catalyzed oxidative free-radical coupling of phenols. We demonstrate the potential of the technique for the polymerization of 8-hydroxyquinoline-5-sulfonate (HQS). Based on the structural changes, we establish the involvement of *ortho*- and *para*-position protons (to the hydroxyl group) in the oxidative free-radical coupling polymerization with their relative preferences. For example, in HQS, we establish that the positions 2, 4, and 7 are involved in the chemical bonding with the order of preference being $7 \geq 2 > 4$. Analyses of ^{13}C-NMR data suggest the formation of C—C- and C—O—C-type coupling bonds during enzymatic polymerization. © 1998 John Wiley & Sons, Inc. J Appl Polym Sci 70: 1257–1264, 1998

Key words: horseradish peroxidase; enzyme-catalyzed polymerization; nuclear magnetic resonance spectroscopy

INTRODUCTION

Horseradish peroxidase-catalyzed polymerization of phenols and anilines has been extensively studied under various experimental conditions such as with aqueous and organic solvents and solvent mixtures, micelles, reverse micelles, and the air–water interface.[1–7] Polymerization of monomers with the help of enzyme-based catalysts are primarily aimed at obtaining controlled molecular weight, molecular organization, and processability of the resulting polymer. Although this reaction is well understood in terms of kinetics, very little is known about the structural changes during polymerization and the precise positions of oxidative coupling.[3]

Spectroscopic techniques have been extensively used to elucidate the kinetics and mechanism of chemical reactions. *In situ* study of structural changes during the chemical reaction will provide vital information for following the mechanism of these reactions.[8] In this report, we discuss the use of *in situ* nuclear magnetic resonance (NMR) spectroscopy to study the biochemical synthesis of polyphenols and polyanilines. Horseradish peroxidase-catalyzed oxidative free-radical coupling of phenols and anilines in the presence of hydrogen peroxide has been studied under various experimental conditions but little is known about the structural changes during polymerization.[1–7]

We monitored the structural changes by *in situ* NMR to unravel the sites that are participating in the oxidative coupling during the polymerization of water-soluble phenol and aniline derivatives.[9] In the present report, we describe the mechanism and the extent of preferences for various sites in

Correspondence to: A. L. Cholli.
Contract grant sponsor: ARO.

Journal of Applied Polymer Science, Vol. 70, 1257–1264 (1998)
 CCC 0021-8995/98/071257-08

the polymerization of 8-hydroxyquinoline-5-sulfonate (HQS). The HQS is shown in the following structure:

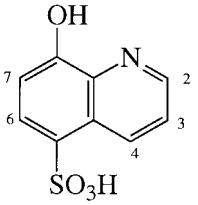

This monomer has five observable protons for NMR, each having a different chemical environment and, therefore, appearing at different chemical-shift values. The monomer is soluble in aqueous medium. Due to the presence of sulfonate groups, the resultant polymer from this monomer is also expected to be soluble in the same solvent. Therefore, this monomer was chosen for the present study. We established site preferences for the oxidative coupling with the help of *in situ* ^{1}H-NMR spectroscopy. In addition, we also discuss the utility of ^{13}C-NMR spectral editing techniques to study the type of chemical bonds present in the final polymer.

EXPERIMENTAL

Horseradish peroxidase was purchased from Sigma Chemicals (St. Louis, MO). HQS and hydrogen peroxide (30%) were purchased from Aldrich Chemicals (Milwaukee, WI). All other chemicals were at least of analytical grade and used as obtained.

All spectrophotometric experiments were carried out using a Perkin–Elmer Lambda 9 UV-vis-near-IR spectrophotometer. *In situ* NMR experiments were carried out using a Bruker DPX 200-MHz NMR spectrometer. Characterization of the monomer and final polymer was carried out using a Bruker ARX 500-MHz NMR spectrometer. The operating frequency on the ARX 500 instrument for performing ^{13}C-NMR and related ^{13}C-NMR experiments was 125 MHz. NMR spectral editing techniques such as distortionless enhanced polarization transfer experiments (DEPT 45, 90, and 135) were also used on the 500-MHz NMR instrument for the identification of —CH_n (n = 1–3) resonances.[10]

Polymer Synthesis

The polymerization of HQS was performed in a 0.1*M* sodium phosphate buffer, pH 7.0. The monomer, 0.2 g, was dissolved in 100 mL of the buffer. One thousand units of the enzyme was added to the buffered monomer solution. The polymerization was initiated by the addition of 20 μL of 30% hydrogen peroxide. The reaction was allowed to continue for 3 h. The solvent was then allowed to evaporate. The resultant polymer was then extracted by first dissolving the reaction product into methanol. The soluble part was separated and methanol was evaporated to obtain a dark yellow-colored solid.

Sample Preparation for *In Situ* Measurements by NMR

Ten milligrams of HQS and 1 unit of horseradish peroxidase in 0.5 mL of 0.2*M* sodium phosphate buffer, pH 7.0, in 99.9% D_2O were added to the NMR for the *in situ* NMR study of enzymatic polymerization. Experimental conditions for the *in situ* NMR study were optimized for acquiring a good-quality spectrum in less than 2 s per experiment.* After collecting the NMR data for the reaction mixture, the reaction was initiated by adding 2 μL of 30% hydrogen peroxide and spectra were recorded within the first minute of the addition of hydrogen peroxide. The experiment was then allowed to continue for about 45 min. During this period, a total of 175 spectra were recorded at fixed time intervals. All spectra were processed under identical conditions.* Spectral characterization of the monomer and the isolated polymer were performed using a Bruker ARX 500-MHz NMR spectrophotometer.[10]

RESULTS AND DISCUSSION

We show the 500-MHz ^{1}H-NMR spectra of the monomer, HQS, and the polymerized HQS, poly-(HQS), in Figure 1(a) and (b), respectively. The resonances due to five protons of the monomer are well resolved, with equal intensity. Assignments of all protons were performed using the contour plot of the COSY-45 experiment (Fig. 2). Cross-peaks in the contour plot were used to assign resonances. The assignments of all proton resonances of HQS are also shown in Figure 2. The

* Number of scans per experiment = 1 (no dummy scans), initial delay (D1) = 10 s, spectral width (SWH) = 602 Hz, SI = 4096, TD = 2048. Acquisition time (AQ) = 1.7 s. RG = 256, O1 = 1601.04 Hz. The data processing was done using a lb of 0.3.

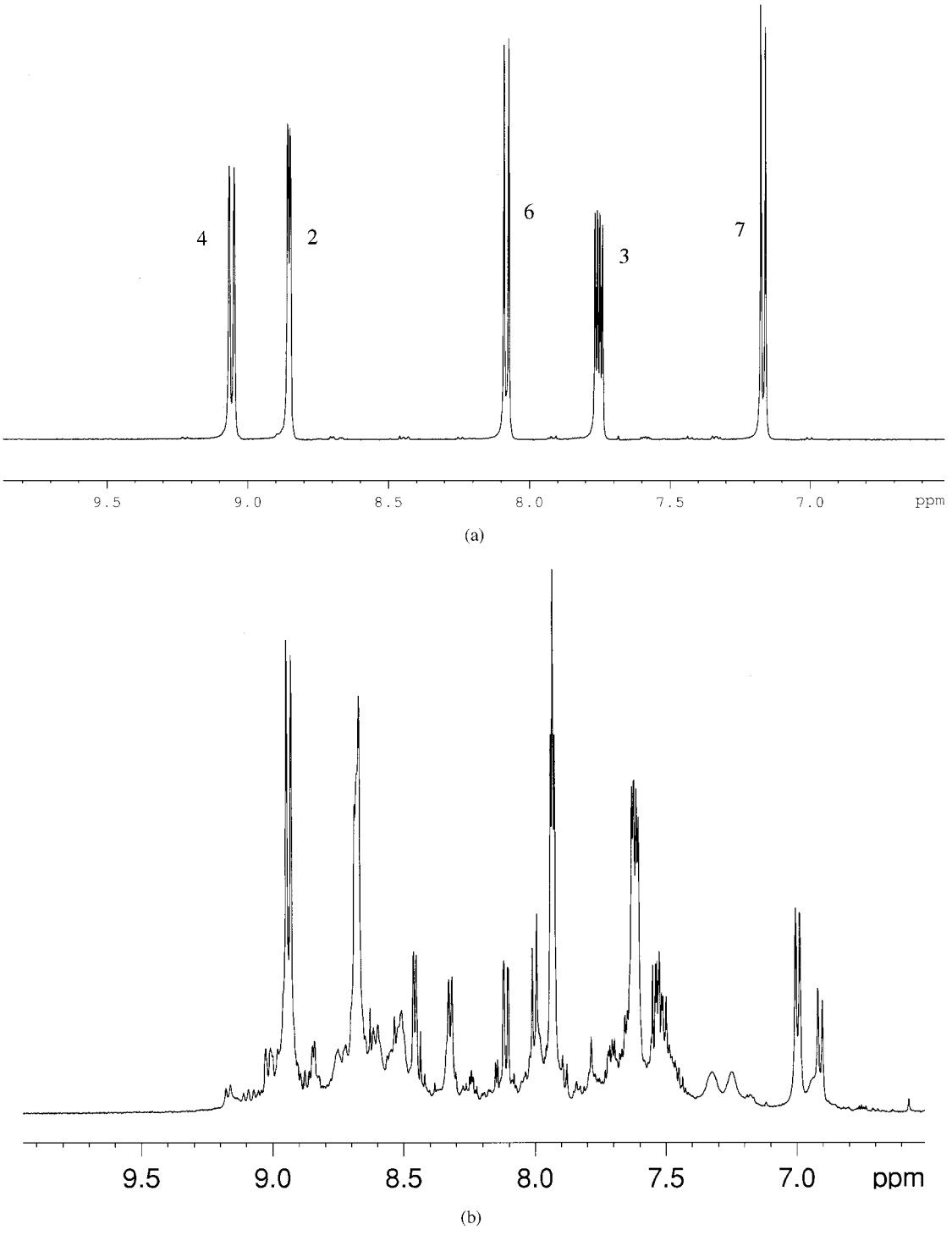

Figure 1 ^{1}H NMR spectrum of (a) HQS and (b) polymerized HQS in D_2O recorded on a 500-MHz NMR instrument.

polymer gives a complex NMR spectrum [Fig. 1(b)]. The characteristic splitting patterns observed in the monomer spectrum are lost in the polymer spectrum due to broadening of the peaks, with the appearance of new peaks including a singlet at 8.8 ppm. Assuming that the coupling occurs at the *ortho* and *para* positions during the enzyme-catalyzed oxidative free-radical coupling

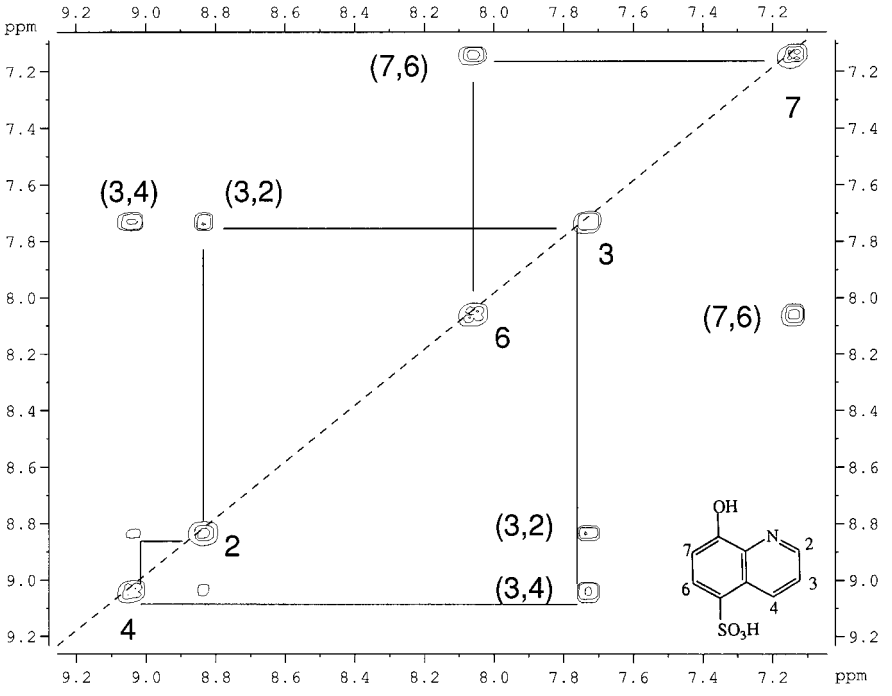

Figure 2 The contour plot of the COSY-45 experiment for the monomer. The assignments of resonances are presented using crosspeaks. See the structure for the numbering of protons.

in HQS, the positions 2, 4, and 7 are expected to participate in the oxidative coupling.[9,11] The new singlet peak (8.8 ppm) in the spectrum of the polymer in Figure 1(b) can be ascribed to the proton at carbon 6 arising due to the coupling at carbon 7. As a result of the coupling reaction at carbon site 7, the chemical shift and the splitting pattern for the neighboring proton at position 6 are expected to be changed. The pattern for proton 6 will change from a doublet to a singlet and will appear at downfield. Similarly, the quartet at 7.5 ppm (proton at carbon 3) should appear as a doublet with a new lower chemical-shift value and its position will be dependent on the position of the coupling (2 or 4). In the cases where both 2 and 4 sites are involved in oxidative coupling, the resonance pattern for proton 3 will change from quartet to singlet. Moreover, the oxidative coupling either at 2 or 4 will also influence on the pattern and position of the resonance for proton 3. In this case, a doublet is expected for proton 3. Additional peaks observed in the region of 7.5 and 8.5 ppm [Fig. 1(b)] therefore arise from the protons at positions 2, 3, and 4 as a result of oxidative couplings at positions 2 and 4. In other words, although the carbons at positions 3 and 6 are not participating directly in the oxidative coupling, their resonances in the ^{1}H-NMR spectrum will appear at different chemical-shift positions due to the neighboring effect. The relative preferences of these three coupling sites (2, 4, and 7) for oxidative coupling is established by following the spectral changes during the initial phase of the polymerization by *in situ* ^{1}H-NMR spectroscopy.

In Situ NMR Spectroscopy

Figure 3 gives a few characteristic spectra recorded on the 200-MHz NMR instrument at different time intervals during the progress of the reaction. The spectral assignment of these peaks is shown in Figure 1(a). As the polymerization progresses, the resonance peaks become broader, their intensities vary with time, and a new peak appears (peak labeled as n) as shown in Figure 3. Additional new resonance peaks were also observed at longer time intervals. The progress of the reaction was monitored by following the change in the integral of the individual peaks as a function of time. The integrals of the peaks in all the spectra were normalized with respect to the HQS peaks in the monomer (at time = 0). The integral of individual peaks is plotted as a function of time in Figure 4. The reaction progresses

rapidly for the first 15–20 min, followed by minor changes thereafter. The noise in the data points is due to the error in the measurement and uncompensated noise in the single-scan spectrum.[10] From Figure 4, it is evident that the protons at positions 2, 4, and 7 are involved in the polymerization reaction. The experimental data suggests that the chemical coupling at position 7 results in the decrease of its peak intensity. This is associated with the change of peak 6 from a doublet to a singlet, with a new chemical-shift value, which is labeled as *n* in spectrum 3. Similarly, the oxidative coupling at positions 2 and 4 result in the change of chemical shift of protons 2, 3, and 4 (from 7.5 to 8.5 ppm). These changes along with the chemical-shift change for proton 6 is labeled as *n* in Figure 3. The total integral of this spectral region is used as an indication of the new resonances arising due to the reaction. Experimental data suggest that positions 2, 4, and 7 are involved in the oxidative coupling. Positions 3 and 6 are not the preferred sites for coupling.[11] From the extent of the decrease in their integrals, it is concluded that positions 2 and 7 are more preferred in the oxidative free-radical coupling reaction than is position 4 due to steric factors. Based on the peak-area changes in Figure 4, the oxidative couplings at various positions follow the order $7 \geq 2 > 4$.

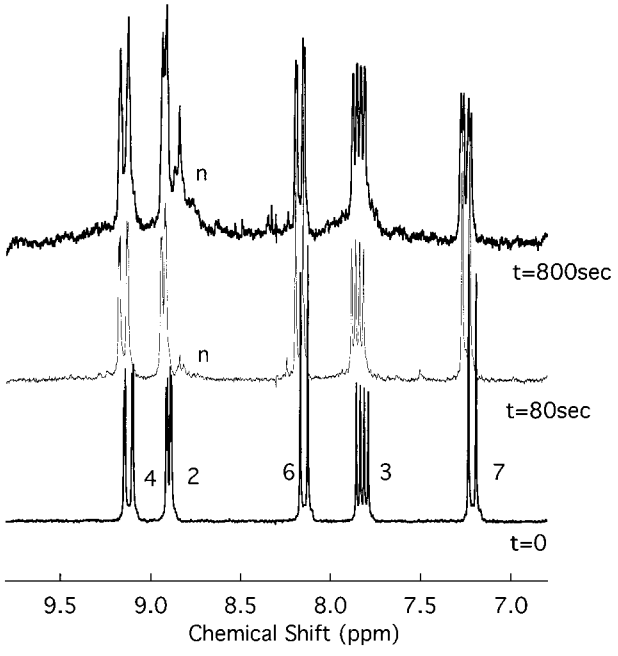

Figure 3 ^{1}H-NMR spectra recorded during the polymerization of HQS at different time interval using a 200-MHz NMR instrument.

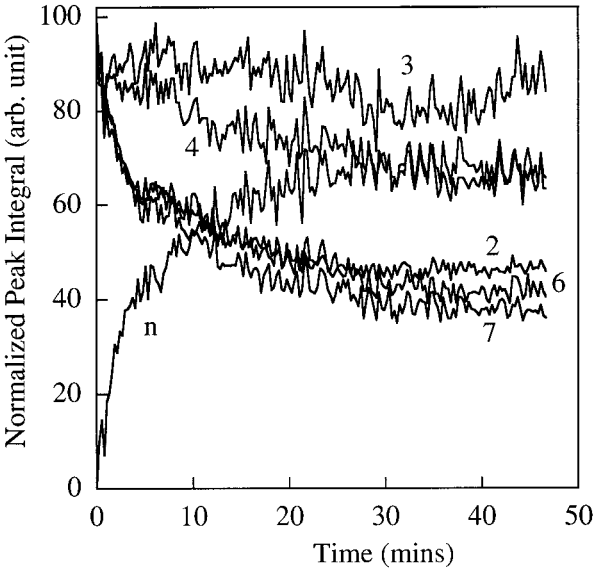

Figure 4 The peak intensities plotted as a function of time for the protons and the new peak (*n*) of HQS from the *in situ* proton NMR spectra.

^{13}C-NMR Data Analysis

The *in situ* ^{1}H-NMR spectrum provides information about the sites involved in the oxidative coupling. However, it does not provide any information on the type of bonds present in the final product. The oxidative free-radical coupling mechanism can result in the formation of bonds C—C, C—O—C, and C—O—O—C (C denotes the parent ring of HQS). ^{13}C-NMR spectroscopy provides direct proof for the existence of these classes of chemical bonds. ^{13}C-NMR, 125-MHz, was used for the additional characterization of this polymer.

^{13}C-NMR and DEPT-90 spectra of the monomer are given in Figure 5. The spectral assignment of the monomer is indicated in the figure. Figure 6 shows the ^{13}C-NMR and DEPT-90 spectrum of the polymer, poly(HQS). Compared with the spectrum for the monomer, the polymer spectrum shows many additional resonance peaks. Although accurate assignments of these additional peaks may not be possible due to the complex nature of the final product, we broadly identify the type of carbons present in the polymer and corresponding resonances with the help of DEPT-90 and DEPT-135 experiments. ^{13}C-DEPT is a commonly used technique for the identification of protonated carbons (—CH_n, n = 1–3). In a typical DEPT-90 spectrum, only the resonances due to methine and methyl carbons are present.

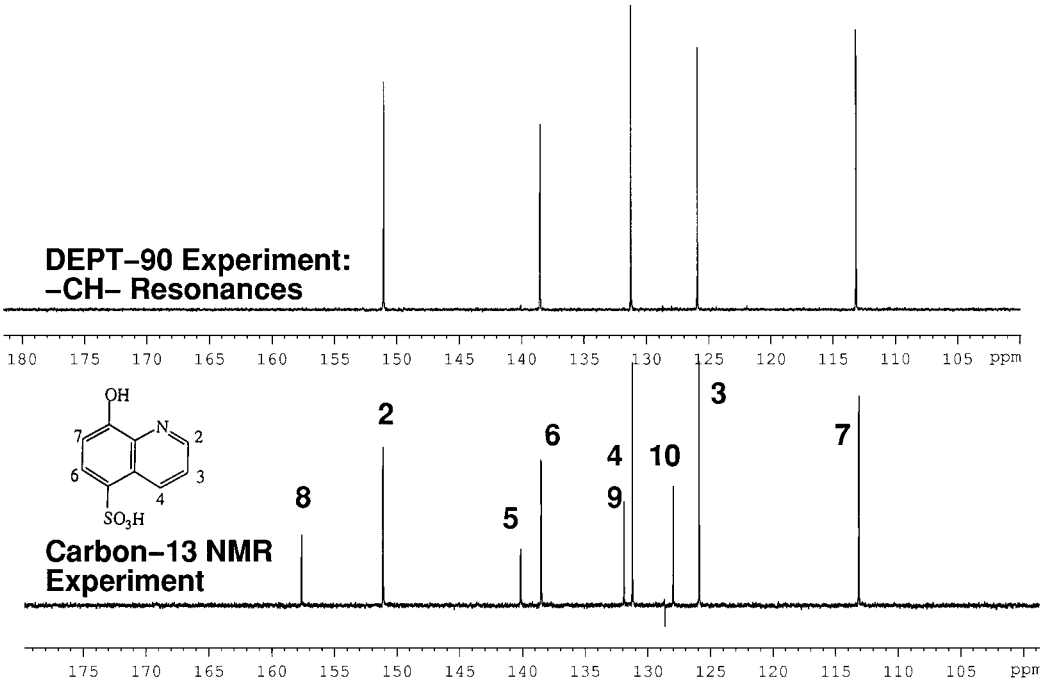

Figure 5 ^{13}C-NMR and DEPT-90 spectra of the monomer in D_2O recorded using a 500-MHz NMR instrument.

In the case of the DEPT-135 spectrum, methylene carbon resonances appear as negative peaks, while the resonances due to methyl and methine carbons, as positive peaks.[10] Figure 6 gives the DEPT-90 spectrum of the polymer. Both the DEPT-90 and DEPT-135 experiments yielded identical spectra; there are no methylene carbons expected in the polymer. Comparing the regular ^{13}C-NMR spectrum with the DEPT spectrum can easily identify the presence of nonprotonated carbons in the polymer. Subtraction of a DEPT spectrum from the regular ^{13}C-NMR spectrum can also provide a spectrum for quaternary carbons in the polymer.

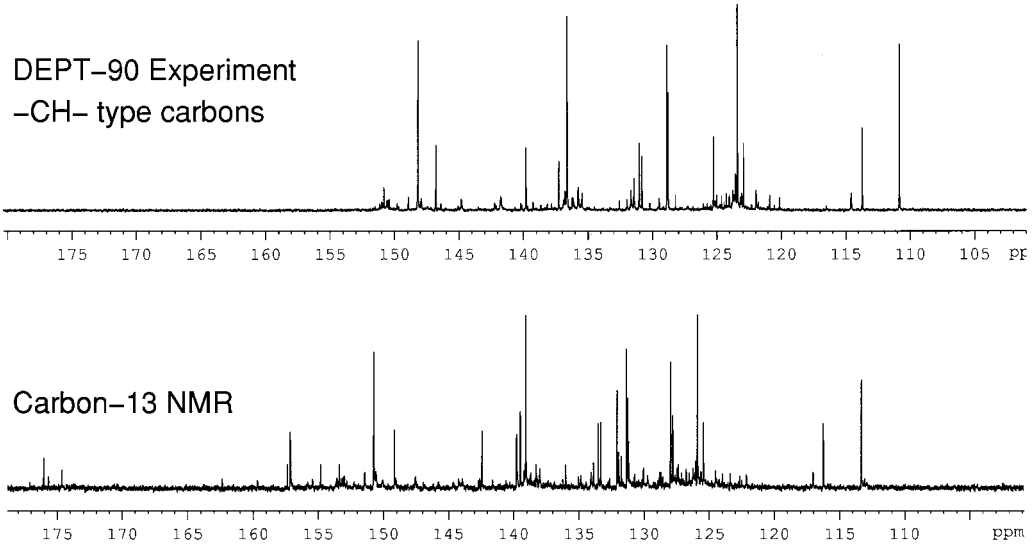

Figure 6 ^{13}C-NMR and DEPT-90 spectra of the polymerized HQS in D_2O recorded using a 500-MHz NMR instrument.

Table I Type of Bonds and Their Expected Resonances Based on the ACD/CNMR Spectral Simulation

CA—CB/CA—O—CB	CA	CB
C2—C2	157	157
C4—C4	146	146
C7—C7	116	116
C2—C4	158	138
C2—C7	154	123
C4—C7	142	122
C8—O—C2	157	158
C8—O—C4	158	160
C8—O—C7	151[a]	140
C8—O—O—C8	154[a]	154

[a] The effect of negatively charged sulfonate groups on the chemical shifts are not accounted for in these calculations.

The ^{13}C-NMR spectrum of the polymer in Figure 6 is complex. It is a difficult task to assign all resonances. Our emphasis was to use NMR data for predicting a general architecture of the polymer system. To provide a generic model for the mechanism, our approach is based on the following steps: (i) identify resonances in the experimental spectrum using spectral editing techniques such as DEPT experiments, (ii) use a semiempirical approach for NMR spectral calculations, and (iii) compare the calculated spectra with the experimental data for the identification of resonances for oxidative coupling carbons. Using ACD/CNMR Labs spectral simulation software, we generated ^{13}C-NMR spectra of the monomer, dimer, and oligomers with possible types of oxidative coupling bonds. The complexity in the calculated spectrum increases with the increasing number of repeat units in the polymer.

C—C Coupling

Six types of carbon–carbon couplings are possible in the oxidative coupling as expected from the proton NMR study. For example, the C7—C7 coupling is expected to appear at ca. 117 ppm, while the coupling C2—C7 will shift the resonance of C7 to 122 ppm and the resonance of C2 will appear at ca. 155 ppm. Carbons involved in the couplings and expected chemical shifts for participating carbons, based on calculated spectra, are listed in Table I.

C—O—C Coupling

C—O—C couplings involve the C8 carbon and any of the C2, C4, or C7 carbons. As presented in Table I, the resonance positions of both carbons will appear downfield and the chemical shifts are dependent on the type of second carbon in the coupled pair. For example, the sulfonate group at the C5 position shifts the resonances of both C8 and C4 more downfield as compared to the coupling at the C7 position. The chemical shifts of some resonances involving C—O—C appear in the 173–177-ppm region. Such a downfield shift for these resonances may be attributed to the effect of negatively charged sulfonic groups on the neighboring carbon C6 participating in the oxidative coupling with other carbons. The software used for the chemical-shift calculation does not take into account the ionic effect on the chemical shifts.

Comparison of the ^{13}C-NMR spectrum with the DEPT-90 spectrum of the polymer and the spectral simulation suggests that there are additional quaternary carbon resonances in the spectral region ca. 120 ppm. These may arise from the C7 carbons coupled to other carbons through C—C coupling. Similarly, quaternary C2 carbon resonances appear ca. 155 ppm and quaternary C4 carbon resonances are ca. 145 ppm. The presence of C—O—C bonds in the polymer is evident from Figure 6. The resonances at ca. 175 ppm are assigned to the C2 and C4 quaternary carbons participating in the C—O—C-type couplings. The resonances of C7 carbons are expected at ca. 140 ppm. This is the first spectroscopic evidence for the presence of such bonds in enzyme-catalyzed polymerization of phenols. Based on the present understanding of the reaction and the spectra, we arrive at the mechanism for the enzymatic polymerization of HQS. Scheme 1 gives the schematic of the mechanism of resonance stabilization of the free radical and the type of bonds present in the final structure.

CONCLUSIONS

In conclusion, *in situ* proton NMR along with ^{13}C-NMR spectroscopy has enabled us to follow the mechanism of enzyme-catalyzed polymerization of HQS. The structural modifications during the polymerization reaction were observed by monitoring the changes in proton resonance intensities. Based on *in situ* NMR data, we were able to identify the site preferences in the polymerization reaction. Experimental data suggest that the *ortho* and *para* positions to the phenolic hydroxyl groups are the preferred sites for the polymerization. In HQS, po-

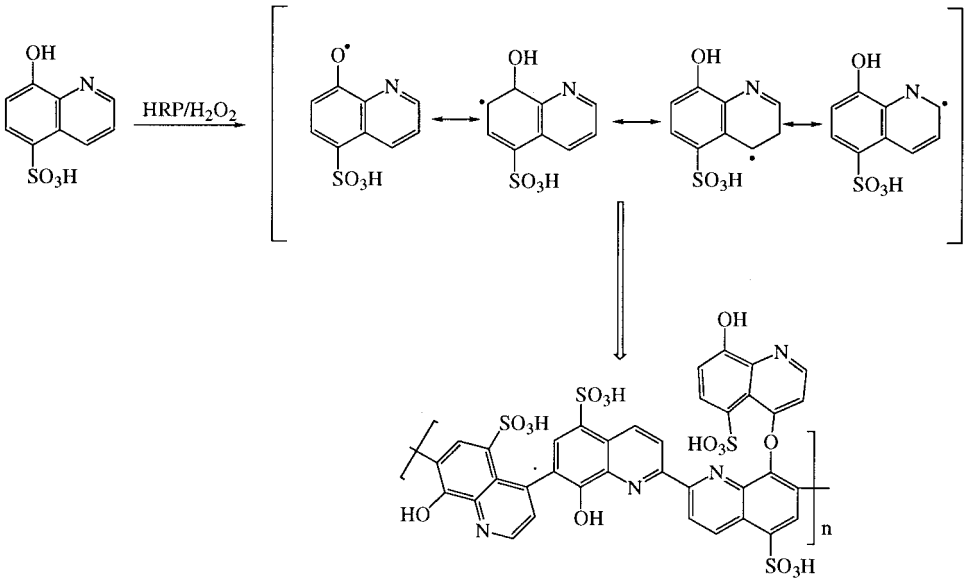

Scheme 1

sitions 2, 4, and 7 are involved in the oxidative free-radical coupling. The lower preference for position 4 as compared to position 2 can be ascribed to the steric hindrance posed by the sulfonate group. The ^{13}C-spectrum supports the existence of C—C as well as of C—O—C bonds in the product. Work is in progress to investigate the enzymatic polymerization of another interesting monomer, aniline, by *in situ* NMR spectroscopy.

One of the authors (K.S.A.) acknowledges the support from ARO. We are also grateful for the use of the NMR facility at the Center for Advanced Materials.

REFERENCES

1. H. Uyama, H. Kurioka, I. Kaneko, and S. Kobayashi, *Macromol. Rep. A,* **31,** 421 (1994).
2. R. Ikeda, H. Uyama, and S. Kobayashi, *Macromolecules,* **29,** 3053 (1996).
3. J. A. Akkara, K. J. Senecal, and D. L. Kaplan, *J. Polym. Sci. A Polym. Chem.,* **29,** 1561 (1991).
4. F. F. Bruno, J. A. Akkara, L. A. Samuelson, D. L. Kaplan, K. A. Marx, J. Kumar, and S. K. Tripathy, *Langmuir,* **11,** 889 (1995).
5. R. Sarma, K. S. Alva, K. A. Marx, S. K. Tripathy, J. A. Akkara, and D. L. Kaplan, *Mater. Sci. Eng. C,* **4,** 189 (1996).
6. F. F. Bruno, K. A. Marx, S. K. Tripathy, J. A. Akkara, L. A. Samuelson, and D. L. Kaplan, *J. Intell. Mater. Syst. Struct.,* **5,** 631 (1994).
7. K. S. Alva, K. A. Marx, J. Kumar, and S. K. Tripathy, *Macromol. Rapid Commun.,* **17,** 859 (1996).
8. A. Hickel, G. Gradnig, H. Griengl, M. Schall, and H. Sterk, *Spectrochem. Acta,* **35,** 3576 (1994).
9. K. S. Alva, K. A. Marx, J. Kumar, and S. K. Tripathy, *Macromol. Rapid Commun.,* **18,** 133 (1997).
10. A. Derome, *Modern NMR Techniques for Chemistry Research,* Pergamon, New York, 1995.
11. C. Walsh, *Enzymatic Reaction Mechanisms,* W. H. Freemand, New York, 1979, pp. 488–493.